Interactions between microtubule-driven membrane protrusions induce filament bundling

A. Vahid and T. Idema

Keywords: cytoskeletal-membrane interactions, filament bundling.

Abstract

The plasma membrane and cytoskeleton of living cells are closely coupled dynamical systems. Internal cytoskeletal elements such as actin filaments and microtubules continually exert forces on the membrane, resulting in the formation of membrane protrusions. In this paper we investigate the interplay between the shape of a cell distorted by pushing and pulling forces generated by microtubules and the resulting rearrangement of the microtubule network. From analytical calculations, we find that two microtubules that deform the vesicle can both attract or repel each other, depending on their angular separations, the size, and the direction of imposed perturbations. We likewise find the necessary conditions for attractive interactions between multiple microtubules. Our results suggest that the commonly reported parallel structures of microtubules in both biological and artificial systems can be a natural consequence of membrane mediated interactions.

Introduction

Cells are enveloped by a plasma membrane which serves as a selective soft physical barrier as well as being home to many functional proteins. The stability and shape of cellular membranes are determined not only by inherent properties of the membrane, but also by interactions with the cell's cytoskeleton (1). The highly dynamic cytoskeletal network is vital for numerous biological processes, including cell motility, cell migration, and cell signaling (2, 3). A typical feature occurring in such processes is the formation of membrane protrusions. Protrusions commonly emerge in the form of microvilli, filopodia or lamellipodia (4, 5). These leading-edge protrusions, the existence of which is vital for responding to external cues, can be driven, controlled and elongated by a complicated crosstalk between the membrane and underlying filaments.

The spatial arrangement of cytoskeletal filaments, force generation mechanisms, and cytoskeletal networks coupling to the shape of cells have been investigated extensively, both theoretically and experimentally (6–10). For example, when growing encapsulated microtubules inside an artificial spherical membrane, it has been shown that the vesicle exhibits a diverse range of morphologies, from a simple elongated shape to dumbbell-like geometries (7). The diversity in the shape of such vesicles results from both the elongation dynamics of the filaments inside them and the material properties of the membrane. Such spatial rearrangement of filaments does not occur spontaneously but stems from the conditions imposed on them from various elements, one of which is the cell shape.

In this paper, we investigate the interplay between the shape of vesicles, that are deformed by internal force generating filaments like microtubules, and the rearrangement of those filaments. In a biological cell, microtubules undergo treadmilling and dynamic instabilities (catastrophes) which are controlled by associated proteins (11). Only a few of the microtubules that grow inside a cell can reach the cell membrane (12). The pushing and pulling forces generated by those few microtubules can be harnessed for creating protrusions of the membrane (13). Membrane mediated interactions between microtubule-induced protrusions may influence the arrangement of other functional filaments in addition to microtubules themselves (14, 15). Therefore, it is warranted to study how the presence of a biological membrane, which has both elastic and fluid properties, alters the interaction between microtubules. This interaction could both drive processes like the formation of filament bundles or inhibit microtubule aggregation.

We use a modified version of the theoretical framework that has been developed for investigating membrane mediated interactions between proteins embedded in or bounded to a fluid membrane (16, 17). We first explain the model in detail. We then study the effects of all the possible elements on the interaction between microtubules. In particular, we demonstrate that changing the in-plane tension in the membrane qualitatively affects the equilibrium shape that a vesicle can adopt. We further reveal that the size and relative orientation of the imposed deformations determines the nature of their interactions. Our results thus elucidate the effective role of the membrane in determining the equilibrium arrangement of protrusions imposed by the cytoskeleton.

Model

We assume that microtubules (including their tip) are rigid and impose sharp deformations on the membrane. To analyze the effect of such perturbations on the shape of an undeformed spherical membrane, we use the conventional Canham-Helfrich bending free energy including fixed surface area (S) and volume (V) constraints, given by:

$$E_{\mathrm{CH}} = \int \mathrm{d}S \left[2\kappa H^2 + \sigma\right] + \Delta P \int \mathrm{d}V \tag{1}$$

with H, σ and ΔP the sum of the two principal curvatures, surface tension and pressure difference, respectively. Due to the conservation of topology we can ignore the Gaussian curvature contribution in the energy functional. Using the spherical analog of the Monge parametrization, we describe the shape of a deformed vesicle as:

$$r(\theta, \phi) = R\left(1 + u(\theta, \phi)\right) \tag{2}$$

where R is the radius of an undisturbed vesicle and $u(\theta, \phi)$ is the deformation field. As the only constraints present are those imposed by the microtubules, we fix the amount of induced deformation at their tip (Fig. 1), $\bar{\mathbf{u}}_0 = (u(\theta_1, \phi_1), \ldots, u(\theta_N, \phi_N))$ with N the number of microtubules. Mathematically, we apply this condition via Lagrange multipliers,

$$E_{\mathrm{MTs}} = \int \mathrm{d}S \left[\mathbf{L} \cdot \left(\bar{\boldsymbol{\delta}}(\Omega - \Omega_0) u(\theta, \phi)\right)\right], \text{where } \bar{\boldsymbol{\delta}}(\Omega - \Omega_0) = \begin{bmatrix} \delta(\Omega - \Omega_1) \\ . \\ . \\ . \\ \delta(\Omega - \Omega_N) \end{bmatrix} \tag{3}$$

where $\mathbf{L}$ is a vector of Lagrange multipliers and $\delta(\Omega - \Omega_i) = \delta\left(\cos(\theta - \theta_i)\right)\delta(\phi - \phi_i)$ is the Dirac delta function for spherical coordinates. In terms of the deformation field and the applied constrains, the total energy of the membrane is given by:

$$\begin{aligned} \frac{E_{\mathrm{Total}}}{\kappa} = \int \mathrm{d}\Omega \Bigg[& 2\left(1 - \nabla^2 u + \frac{1}{4}(\nabla^2 u)^2 + u\nabla^2 u + \frac{1}{2}|\nabla u|^2\right) \\ & + \bar{\sigma}\left((1+u)^2 + \frac{1}{2}|\nabla u|^2\right) - \frac{\overline{\Delta P}}{3}(1+u)^3 - \mathbf{L} \cdot (\bar{\boldsymbol{\delta}} u)\Bigg], \end{aligned} \tag{4}$$

where the nondimensionalized surface tension and pressure difference are defined as $\bar{\sigma} = \frac{R^2\sigma}{\kappa}$ and $\overline{\Delta P} = \frac{R^3 \Delta P}{\kappa}$, respectively. In the small deformation regime, we can approximate the relative behavior of the pressure difference and surface tension as that of the Laplace pressure for a sphere: $\overline{\Delta P} = 2\bar{\sigma}$. We then obtain the linearized form of the shape equation by minimizing Eq. 4, which gives:

$$\nabla^2\nabla^2 u + (2 - \bar{\sigma})\nabla^2 - 2\bar{\sigma} u = \mathbf{L}.\bar{\boldsymbol{\delta}} \tag{5}$$

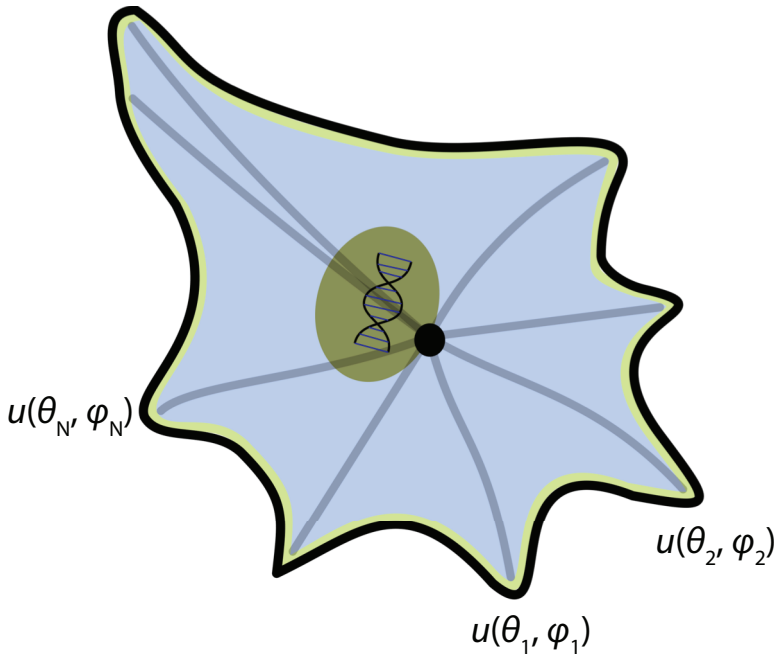

Figure 1: Schematic shape of a cell containing some microtubules. We model the microtubules by the imposed deformation ($\bar{\mathbf{u}}_0 = (u(\theta_1, \phi_1), \ldots, u(\theta_N, \phi_N))$) at their tips.

Because the resultant equation is linear, the final solution for the deformation field of the membrane can be constructed as:

$$u(\theta, \phi) = \mathbf{L} \cdot \bar{\mathbf{g}}(\Omega - \Omega_0), \text{where } \bar{\mathbf{g}}(\Omega - \Omega_0) = \begin{bmatrix} G(\Omega - \Omega_1) \\ . \\ . \\ . \\ G(\Omega - \Omega_N) \end{bmatrix}. \tag{6}$$

In these equations $G(\Omega - \Omega_i)$ is the Green's function of the left hand side of Eq. 5. We expand the Dirac delta function in terms of spherical harmonics[1], and solve for the Green's function, which gives:

$$G(\theta - \theta', \phi - \phi') = \sum_{l=2}^{\infty} \sum_{m=-l}^{l} \frac{Y_l^m(\theta, \phi) Y_l^{m*}(\theta', \phi')}{l^2(l+1)^2 - (2 - \bar{\sigma}) l(l+1) - 2\bar{\sigma}}. \tag{7}$$

In Eq. 7 we have excluded the first two modes. The zeroth mode corresponds to motion of the center of mass. Excluding the first mode is necessary to prevent inflation of the vesicle, as we have already penalized any changes in the volume in Eq. 4. Excluding these modes implies correcting the Dirac delta in Eq. 5, which is reasonable for small deformations. Finally, taking into account the constraints associated with the microtubules (the vector $\bar{\mathbf{u}}_0$),

[1] $\delta(\phi - \phi')\delta(\cos(\theta - \theta')) = \sum_{l=0}^{\infty} \sum_{m=-l}^{l} Y_l^m(\theta, \phi) Y_l^{m*}(\theta', \phi')$, where the symbol '*' denotes complex conjugate.

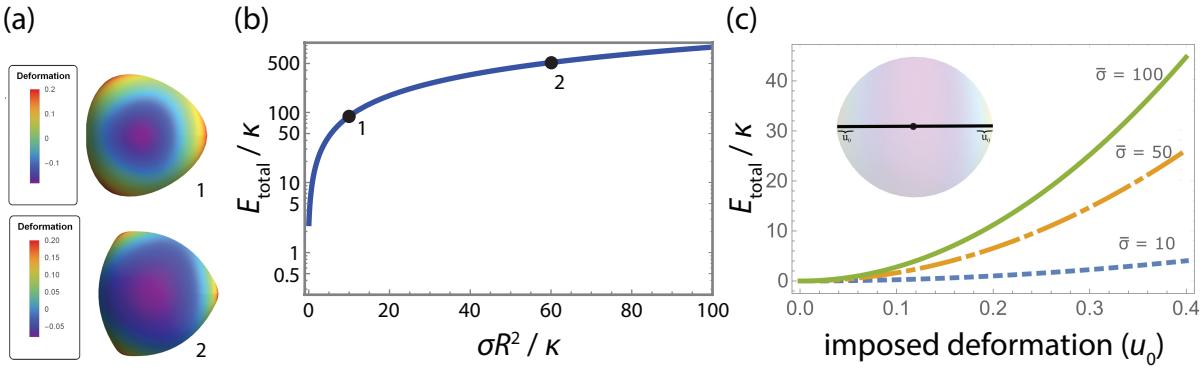

Figure 2: Membrane deformation due to the presence of microtubules. (a) Snapshots of a deformed vesicle for low (1) and high (2) values of the surface tension. The imposed deformation vector reads $\bar{\mathbf{u}}_0 = (0.1, 0.1, 0.1)$. (b) Increasing the in-plane tension makes the membrane deformation more spiky, in contrast to low surface tension regimes where we have rounded deformations. Numbers correspond to the images in (a). (c) The deformation energy of a spherical membrane containing two growing microtubules for different values of the surface tension.

we obtain the Lagrange multipliers and the induced deformation field as:

$$\mathbf{L} = \bar{\mathbf{u}}_0^T \cdot \mathbf{M}^{-1}, \text{ and } u(\theta, \phi) = \bar{\mathbf{u}}_0^T \cdot \mathbf{M}^{-1} \cdot \bar{\mathbf{g}}(\Omega - \Omega_0), \tag{8}$$

where $\mathbf{M}$ is an $N \times N$ matrix whose components are constructed as $m_{ij} = G(\theta_i - \theta_j, \phi_i - \phi_j)$, with $i = 1, \ldots, N$ and $j = 1, \ldots, N$. For the diagonal components of the matrix $\mathbf{M}$ (when $i = j$, corresponding to self-interactions), because we have a constant number of lipids and the vesicle is closed, we consider a maximum mode $l = L_{\max}$ in Eq. 7. Substituting the derived deformation field $u(\theta, \phi)$ in Eq. 4, one can get the total energy of the membrane as:

$$\frac{E_{\text{Total}}}{\kappa} = \frac{1}{2}\bar{\mathbf{u}}_0^T \cdot \mathbf{M}^{-1} \cdot \bar{\mathbf{u}}_0 + 8\pi \left(1 + \frac{\bar{\sigma}}{3}\right). \tag{9}$$

Given an arbitrary number of microtubules, all we need is the amount of deformation they impose to investigate their interactions. The only relevant length scale of our system relates surface tension to the bending modulus, given by $\lambda = \sqrt{\kappa/\sigma}$. In a biological context, the pertinent values of λ are in the range of $60 - 100$ nm (18, 19). Given this length scale, one can obtain the nondimesionalized physiologically relevant values of surface tension as: $\bar{\sigma} = (R/\lambda)^2$. For a value of $\lambda = 100$ nm, for example, we get $\bar{\sigma} = 100$ for a vesicle size of $R = 1$ μm.

To examine the effect of surface tension on the equilibrium shape of the membrane, we position three microtubules inside a vesicle such that they form an equilateral triangle, and all impose the same amount of deformation on the membrane ($u_0 = 0.1$). For small values of $\bar{\sigma}$, we are in a bending dominated regime. The membrane, therefore, minimizes the total mean curvature, as illustrated in Fig. 2a. Increasing $\bar{\sigma}$ alters the local shape of membrane

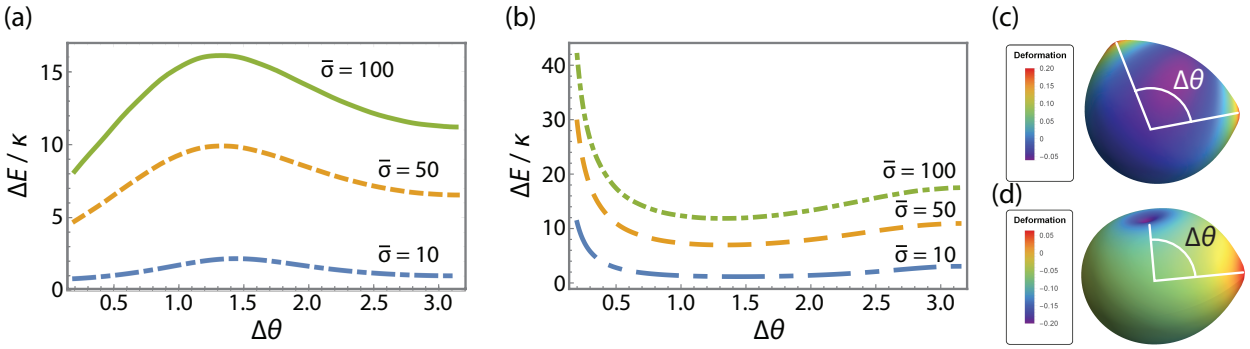

Figure 3: The interaction between microtubule-driven protrusions. (a) Microtubules that deform the membrane identically, attract each other and bundle for separations smaller than a critical angle $\Delta\theta_c \simeq 5\pi/12$. The elastic nature of the membrane hinders microtubule coalescence for larger separations. (b) Protrusions of opposite orientation repel each other for small distances and attract for large angular separations. Right panel: Snapshots of two protrusions that are imposed either identically (c) or oppositely (d).

at the tip of microtubules from being smoothly curved into sharp spikes with higher total energy (Fig. 2b). Next, we analyze the total energy of a vesicle encapsulating two growing microtubules that push the membrane in opposite directions (Fig. 2c). We assume that the two microtubules distort the membrane similarly. As expected, the more a vesicle elongates, the larger the stored energy becomes. Also, membrane vesicles with a high in-plane tension require more energy to initiate a protrusion process. Microtubules are dynamic entities and constantly switch between growing and shrinking phases that are characterized by rescue and catastrophe events (20). Not only are they able to generate a pushing force during growing into obstacles like membrane, microtubules can also release a force in the course of shrinking, which can be harnessed for pulling purposes (in case of deformable obstacles). The pushing forces are in the range of $2-3$ pN (21), leading to an energy of $40-60$ κ for a deformation[2] of $u_0 = 0.1$. Therefore, having membrane protrusions that cost a total energy (E_{Total}) of not more than $60-100$ κ would still allow tubulin dimers to aggregate at the end of the microtubules. The depolymerization-dependent forces are about one order of magnitude stronger ($\sim 30-65$ pN (22)) than those generated during the growth state. Therefore, the force numbers in the biological context are high enough to impose distortions of a similar size as we suppose in our calculations – although depending on the length of the microtubules, some processes like buckling may decrease the maximum force they exert on the membrane.

The arrangement of filaments plays a key role in the emergent shape of protrusions and consequently in sensing the extracellular environment. To unravel the nature of elastic interaction between protrusions, we investigate a vesicle containing two protrusions with a varying angular separation between them. For identical deformations, as illustrated in Fig. 3, we have both short-range attraction and long-range repulsion regimes, that are

[2]We assume a bending modulus of $\kappa = 25 k_B T$ for the membrane and a vesicle size of 1 μm.

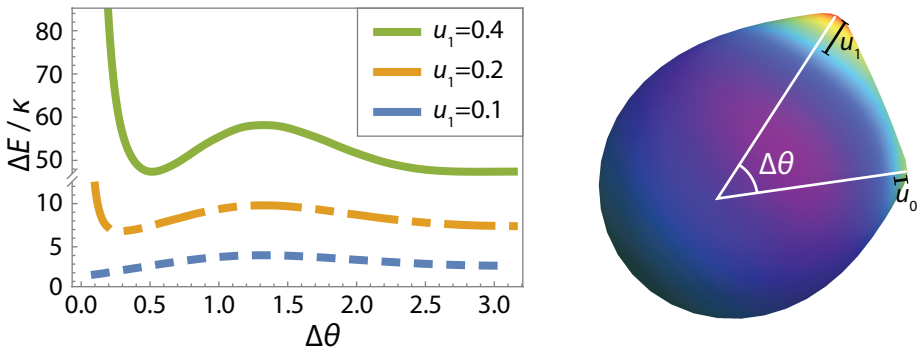

Figure 4: Interaction between microtubule-driven protrusions of different strength. As shown in the graph, introducing a difference in the magnitude of the protrusions results in a very strong short range repulsion between them ($u_0 = 0.1$; $\bar{\sigma} = 10$).

connected at a critical angle $\theta_c = 5\pi/12$. The plot suggests that cellular membranes facilitate the aggregation of microtubules for short separations and hinder their assembly for longer distances. Although the global minimum of the energy is when two protrusions are merged, there is an energy barrier, the value of which increases with the surface tension. Inversely, two oppositely oriented protrusions repel each other for short and attract for larger distances. When analyzing the interaction between protrusions of different sizes, we realize that altering the magnitude of deformation for one of the microtubules strikingly changes the nature of interactions in their small separations. For example, as illustrated in Fig. 4, making one of the constraints stronger/weaker than the other turns short range attraction into repulsion. This suggests that having such distortions on a vesicle is costly, and that cells will therefore try to minimize the amount of deformed material between them by adjusting their protrusions. Putting the results of the two previous experiments together, we find that when interacting with membranes, microtubules rearrange themselves in such a way to form parallel filaments. Such rearrangements are ubiquitous in cells, for instance in the early stages of filopodia. Our results therefore suggest that these phenomena can be a natural result of membrane mediated interactions between microtubules.

Our system easily extends to vesicles that contain more than two microtubules, with similar results. To illustrate this point, we plot the whole configuration space for the case of three microtubules (Fig. 5) to look for the possible (semi) stable configurations. It turns out that the global minimum of the resultant energy landscape is when all the microtubules are attached to each other. There are, however, some local minima, all of which correspond to the situation where two microtubules are bundled together and the other points to the opposite pole of the vesicle.

Conclusion

Together with actin and intermedediate filaments, microtubules form an architecture that governs the shape of a cell, and therefore that of the plasma membrane surrounding it. The

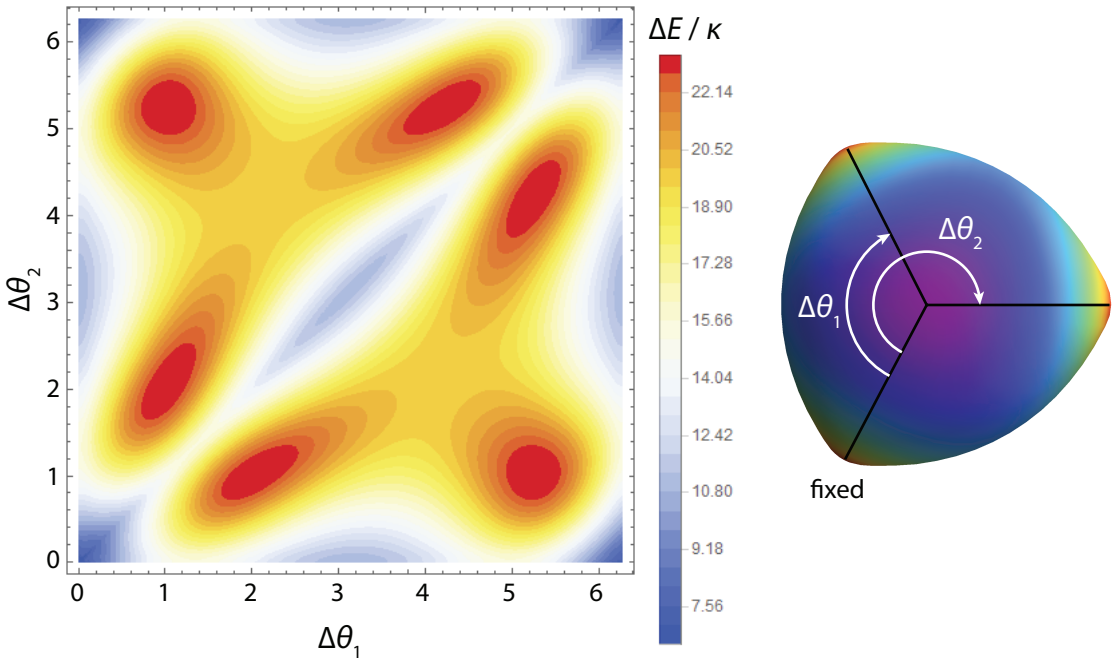

Figure 5: Plot of the configuration space of a vesicle with three enclosed microtubules, with the energy of each configuration shown in color. The closed shape of the vesicle favors the formation of parallel structures of microtubules. The global minimum of the energy corresponds to the situation where all the filaments are bundled, with local minima for the case of having two tubules together and one pointing in the opposite direction. Because filaments polymerize from the centrosome in opposite directions, the local minima may be biologically relevant.

membrane, in turn, mediates the interaction between attached microtubules. Using analytical tools, we studied the effect of membrane mediated interactions on the rearrangement of microtubules. Our results suggest that the elastic properties of cellular membranes facilitate the bundling of microtubules. In particular, we showed that two vesicle-encapsulated microtubules attract each other for small angular separations and repel for large angles. As we explicitly demonstrated for three microtubules, the outcome of collective interactions between multiple filaments is microtubule coalescence, which may be harnessed for protrusion formation (23). Our results reveal that force generating microtubules, when colliding with a deformable obstacle like a fluid membrane, can coordinate their growing state through the shape of distorted membrane between them. Putting all the results together, our study suggests a possible mechanism underlying the preference of filaments for organizing in parallel configurations (24).

Acknowledgments

This work was supported by the Netherlands Organisation for Scientific Research (NWO / OCW), as part of the Frontiers of Nanoscience program.

References

[1] Fletcher, D. A., and R. D. Mullins. 2010. Cell mechanics and the cytoskeleton. *Nature*. 463:485.

[2] Revenu, C., R. Athman, S. Robine, and D. Louvard. 2004. The co-workers of actin filaments: from cell structures to signals. *Nature reviews. Molecular cell biology*. 5:635.

[3] Lodish, H., A. Berk, S. L. Zipursky, P. Matsudaira, D. Baltimore, and J. Darnell. 2000. The actin cytoskeleton. WH Freeman.

[4] Ridley, A. J. 2006. Rho gtpases and actin dynamics in membrane protrusions and vesicle trafficking. *Trends in Cell Biology*. 16:522–529.

[5] Le Clainche, C., and M.-F. Carlier. 2008. Regulation of actin assembly associated with protrusion and adhesion in cell migration. *Physiological Reviews*. 88:489–513.

[6] Fygenson, D. K., J. F. Marko, and A. Libchaber. 1997. Mechanics of microtubule-based membrane extension. *Physical Review Letters*. 79:4497.

[7] Emsellem, V., O. Cardoso, and P. Tabeling. 1998. Vesicle deformation by microtubules: a phase diagram. *Physical Review E*. 58:4807.

[8] Mesarec, L., W. Góźdź, S. Kralj, M. Fošnarič, S. Penič, V. Kralj-Iglič, and A. Iglič. 2017. On the role of external force of actin filaments in the formation of tubular protrusions of closed membrane shapes with anisotropic membrane components. *European Biophysics Journal*. 46:705–718.

[9] e Silva, M. S., J. Alvarado, J. Nguyen, N. Georgoulia, B. M. Mulder, and G. H. Koenderink. 2011. Self-organized patterns of actin filaments in cell-sized confinement. *Soft Matter*. 7:10631–10641.

[10] Atilgan, E., D. Wirtz, and S. X. Sun. 2006. Mechanics and dynamics of actin-driven thin membrane protrusions. *Biophysical Journal*. 90:65–76.

[11] Kerssemakers, J. W., E. L. Munteanu, L. Laan, T. L. Noetzel, M. E. Janson, and M. Dogterom. 2006. Assembly dynamics of microtubules at molecular resolution. *Nature*. 442:709.

[12] Howard, J., and A. A. Hyman. 2003. Dynamics and mechanics of the microtubule plus end. *Nature*. 422:753.

[13] Liu, M., V. C. Nadar, F. Kozielski, M. Kozlowska, W. Yu, and P. W. Baas. 2010. Kinesin-12, a mitotic microtubule-associated motor protein, impacts axonal growth, navigation, and branching. *Journal of Neuroscience*. 30:14896–14906.

[14] Svitkina, T. M., E. A. Bulanova, O. Y. Chaga, D. M. Vignjevic, S. Kojima, J. M. Vasiliev, and G. G. Borisy. 2003. Mechanism of filopodia initiation by reorganization of a dendritic network. *J. Cell Biol.* 160:409–421.

[15] Conde, C., and A. Cáceres. 2009. Microtubule assembly, organization and dynamics in axons and dendrites. *Nature reviews. Neuroscience*. 10:319.

[16] Dommersnes, P. G., and J.-B. Fournier. 2002. The many-body problem for anisotropic membrane inclusions and the self-assembly of saddle defects into an egg carton. *Biophysical Journal*. 83:2898–2905.

[17] Vahid, A., and T. Idema. 2016. Pointlike inclusion interactions in tubular membranes. *Physical Review Letters*. 117:138102.

[18] Evans, A., M. Turner, and P. Sens. 2003. Interactions between proteins bound to biomembranes. *Physical Review E*. 67:041907.

[19] Dai, J., and M. P. Sheetz. 1999. Membrane tether formation from blebbing cells. *Biophysical Journal*. 77:3363–3370.

[20] Bowne-Anderson, H., M. Zanic, M. Kauer, and J. Howard. 2013. Microtubule dynamic instability: a new model with coupled gtp hydrolysis and multistep catastrophe. *Bioessays*. 35:452–461.

[21] Dogterom, M., and B. Yurke. 1997. Measurement of the force-velocity relation for growing microtubules. *Science*. 278:856–860.

[22] Grishchuk, E. L., M. I. Molodtsov, F. I. Ataullakhanov, and J. R. McIntosh. 2005. Force production by disassembling microtubules. *Nature*. 438:384.

[23] Weichsel, J., and P. L. Geissler. 2016. The more the tubular: Dynamic bundling of actin filaments for membrane tube formation. *PLoS Computational Biology*. 12:e1004982.

[24] Liu, A. P., D. L. Richmond, L. Maibaum, S. Pronk, P. L. Geissler, and D. A. Fletcher. 2008. Membrane-induced bundling of actin filaments. *Nature Physics*. 4:789.